anteroposterior, ±2.0 mm mediolateral from the bregma, -1.5 mm dorsoventral from the skull) according to the atlas of Paxinos and Franklin (2004). A dummy cannula (0.3 mm in diameter; Eicom) was left in place throughout the experiment. Five days after the operation, mice were subjected to the novel object recognition test or conditioned fear learning test.

Drug treatment

Cyclosporine A (CsA) obtained from Novartis Pharmaceuticals (Basel, Switzerland) was dissolved in ethyl alcohol/polyethoxylated castor oil (35/65). For microinjection into the hippocampus, a 28-gauge injection cannula (Eicom) cut to extend 1.0 mm beyond the guide cannula was inserted through the guide cannula. Among the known targets of CsA, Cyp D has one of the lowest Ki values in vitro (Galat, 1993). However, one specific concern with the use of CsA to block Cyp D is the possibility of inhibition of the protein phosphatase, calcineurin. Levy et al have reported high doses (250 μM) of CsA inhibit calcineurin in the hippocampal slice by measuring the phosphorylation state of a calcineurin substrate, synapsin I (2003). Considering with these reports and diffusion of CsA in hippocampus, CsA was diluted with artificial cerebrospinal fluid (CSF: 147 mM NaCl, 4 mM KCl and 2.3 mM $CaCl_2$) at a concentration of 100 μM and injected bilaterally (100 pmol/1.0 μl/side) over a 5-min period 10 min before the training session in the novel object recognition test or the conditioning session in the conditioned fear learning test.

Behavioral analysis

A battery of behavioral experiments was carried out according to previous reports

(Mouri et al., 2007a). The behavioral tests were carried out sequentially with the Y-maze test, Novel-object recognition test, Morris water maze test and Cued and contextual fear conditioning tests.

Spontaneous alternation in a Y-maze test

The maze was made of black painted wood; each arm was 40 cm long, 12 cm high, 3 cm wide at the bottom, and 10 cm wide at the top. The arms converged at an equilateral triangular central area that was 4 cm at its longest axis. Each mouse was placed at the center of the apparatus and allowed to move freely through the maze during an 8-min session. The series of arm entries was recorded visually. Alternation was defined as successive entry into the three arms, on overlapping triplet sets. The alternation behavior (%) was calculated as the ratio of actual alternations to possible alternations (defined as the number of arm entries minus two), multiplied by 100.

Novel-object recognition test

The test procedure consisted of three sessions: habituation, training, and retention. Each mouse was individually habituated to the Plexiglas box (30 x 30 x 35 high cm), with 10 min of exploration in the absence of objects for 3 days (habituation session). During the training session, two objects were placed in the back corner of the box. The objects were a golf ball, wooden cylinders, and square pyramids, which were different in shape and color but similar in size. A mouse was then placed midway at the front of the box and the total time spent exploring the two objects was recorded for 10 min. An animal was considered to be exploring the object when its head was facing the object or it was touching or sniffing the object. During the retention session,

the animals were placed back into the same box 24 h after the training session, in which one of the familiar objects used during training was replaced with a novel object. The animals were then allowed to explore freely for 10 min and the time spent exploring each object was recorded. Throughout the experiments, the objects were used in a counterbalanced manner in terms of their physical complexity and emotional neutrality. A preference index, a ratio of the amount of time spent exploring any one of the two objects (training session) or the novel object (retention session) over the total time spent exploring both objects, was used to measure cognitive function.

Morris water maze test

The Morris water maze test was conducted in a circular pool 1.2 m in diameter and filled with water at a temperature of 22 ± 1°C. A hidden platform (7 cm in diameter) was used. The mice were given two trials (one block), 60 sec each trial, for 10 consecutive days during which the platform was left in the same position. The time taken to reach to the escape platform (escape latency) was determined in each trial by using the Etho Vision system (Brainscience idea Co. Ltd., Osaka, Japan). Three hours after the last training trial, the mice were given a probe test without the platform, and were allowed 60 sec to search the pool.

Cued and contextual fear conditioning tests

For measuring basal levels of freezing response (preconditioning phase), mice were individually placed in a neutral cage (17 x 27 x 12.5 high cm) for 1 min, and then in the conditioning cage (25 x 31 x 11 high cm) for 2 min. For training (conditioning phase), mice were placed in the conditioning cage, and then a 15-sec tone (80 dB) was delivered

as a conditioned stimulus. During the last 5 sec of the tone stimulus, a foot shock of 0.6 mA was delivered as an unconditioned stimulus through a shock generator (Brainscience idea Co. Ltd.). This procedure was repeated four times with 15-sec intervals. Cued and contextual tests were carried out 1 day after fear conditioning. For the cued test, the freezing response was measured in the neutral cage for 1 min in the presence of a continuous-tone stimulus identical to the conditioned stimulus. For the contextual test, mice were placed in the conditioning cage, and the freezing response was measured for 2 min in the absence of the conditioned stimulus.

Western blot analysis

Western blotting was performed as previously described (Mouri et al., 2007b). The mice were sacrificed by decapitation, and the brain was immediately removed. The hippocampus was rapidly dissected out on an ice-cold plate, frozen, and stored at –80 °C until used. To prepare tissue extracts, the dissected brain tissue was homogenized by sonication in an ice-cold lysis buffer (20 mM Tris-HCl (pH 7.4), 150 mM NaCl, 50 mM NaF, 2 mM EDTA, 0.1% sodium dodecyl sulfate (SDS), 1% sodium deoxycholate, 1% NP-40, 1 mM sodium orthovanadate, 20 μg/ml pepstatin, 20 μg/ml aprotinin, and 20 μg/ml leupeptin). The homogenate was centrifuged at 13,000 x g for 20 min and the supernatant was used. The protein concentration was determined using a DC Protein Assay Kit (Bio-rad, Richmond, CA). Samples (10-100 μg of protein) were boiled in sample buffer (125 mM Tris-HCl pH 6.8, 10 % 2-mercaptoethanol, 4 % sodium diphosphate decahydrate, 10 % sucrose, and 0.004 % bromophenol blue), separated on a polyacrylamide gel, and subsequently transferred to polyvinylidene difluoride (PVDF) membranes (Millipore Corporation, Billerica, MA). The membranes were blocked

with a Detector Block Kit (Kirkegaard and Perry Laboratories, Gaithersburg, MD) and probed with a primary antibody. Membranes were washed with the washing buffer [50 mM Tris-HCl (pH 7.4), 0.05 % Tween 20, and 150 mM NaCl] and subsequently incubated with a horseradish peroxidase-conjugated secondary antibody. The immune complexes were detected based on chemiluminescence (ECL kit, Amersham Biosciences, Piscataway, NJ) and exposed to X-ray film (Hyperfilm, Amersham Biosciences). The band intensities on the film were analyzed by densitometry using the ATTO Densitograph Software Library Lane Analyzer (ATTO, Tokyo, Japan). To confirm equal loading of each protein, membranes were stripped with stripping buffer [100 mM 2-mercaptoehanol, 2 % SDS, and 62.5 mM Tris-HCl (pH6.7)] at 50 °C for 30 min, and GAPDH protein expression was detected as described above.

The primary antibodies were, a rabbit anti-CyP D (1:1000; synthesized by the authors using a peptide (aa43 to 57) of Cyp D), a mouse anti-MAP2 (1:1000; Chemicon, Temecula, CA), a rabbit anti-growth associated protein (GAP)-43 (1:1000; Chemicon), a mouse anti-glial fibrillary acidic protein (GFAP) (1:1000; Chemicon), a rabbit anti-synaptophysin (1:1000; Dako, Glostrup, Denmark), a guinea pig anti-glutamate transporter GLAST and a guinea pig anti-GLT-1 (1:1000; Chemicon), a mouse anti-glutaminase (GLS) (1:500; Abnova, Taipei, Taiwan), a mouse anti-NR1 CT (1:1000; Upstate Biotechnology, Lake Placid, NY), a mouse anti-NMDAR2A and a mouse anti- NMDAR2B (1:1000; BD PharMingen, San Diego, CA), a rat anti-ChAT (Calbiochem, San Diego, CA) and a goat anti-ACHE (E-19) (1:500 ; Santa Cruz Biotechnology, Santa Cruz, CA). The secondary antibodies, used at a dilution of 1:2000, were horseradish peroxidase-linked anti-mouse, anti-rabbit, anti-rat or anti-guinea pig IgG (Kirkegaard and Perry Laboratories).

Preparation of brain slice and staining

Histological procedures were performed as previously described with a minor modification (Murai et al., 2007). Mice were anesthetized with chloral hydrate (150 mg/kg i.p.) and perfused transcardially with ice-cold phosphate-buffered saline (PBS), followed by 4% paraformaldehyde in PBS. The brains were removed, postfixed in the same fixative for 2 h, and then soaked in 20% (w/v) sucrose in PBS. Coronal sections 15 μm thick were cut with a Cryostar HM560 cryostat (Microm International, GmbH, Walldorf, Germany). For immunohistochemistry, the primary antibodies that were applied in the brain slices included a rabbit anti-Cyp D (1:500; synthesized by the authors), a mouse anti-neuron-specific nuclear antigen (NeuN) (1:500; Chemicon) and mouse anti-GFAP (1:500; Chemicon) antibody. Fluorescently conjugated secondary antibodies (Alexa 488, 546, Invitrogen, Carlsbad, CA) were used for detecting chromagen. For Nissl staining, sections were cut at 40 μm intervals and staining was done according to standard procedures (Murai et al., 2007). Images were acquired with a confocal microscope (LSM510; Carl Zeiss, Jena, Germany) and a light microscope (Axiocam HRc; Carl Zeiss).

In vivo microdyalysis

In vivo microdialysis was performed as previously described (Mouri et al., 2007b; Murai et al., 2007). Mice were anesthetized with sodium pentobarbital (40 mg/kg i.p.) before the stereotaxic implantation of a guide cannula (AG-6, Eicom, Kyoto, Japan) into the ventral hippocampus (-2.8 mm anteroposterior, ±3.0 mm mediolateral from the bregma, -2.0 mm dorsoventral from the skull). One day after the operation, a dialysis

probe (AI-4-2; 2 mm membrane length, Eicom) was inserted through the guide cannula and perfused with CSF (147 mM NaCl, 4 mM KCl and 2.3 mM CaCl2) at a flow rate of 1 µl/min. The dialysate was colleted every 20 min. Dialysates were assayed by HPLC with electrochemical detection (HTEC-500, Eicom) under the following conditions. Three samples were taken to establish baseline levels of extracellular neurotransmitter. For depolarization stimulation, 50 mM KCl-containing Ringer solution was delivered through the dialysis probe for 20 min in order to induce the K^+-evoked release of glutamate and acetylcholine. Then dialysate was collected for 20min with ringer solution.

Statistic analysis

All results were expressed as the mean ± s.e.m. for each group. The difference between groups was analyzed with a one-way, two-way, or repeated ANOVA, followed by the Bonferroni/Dunn multiple range-test. The Student t-test was used to compare two sets of data.

Results

General characteristics of Cyp D $^{-/-}$ mice

The genotype for the Cyp D locus was assessed by PCR (Fig. 1A). Cyp $D^{-/-}$ mice were confirmed to lack Cyp D protein by western blotting (Fig. 1B). Cyp $D^{-/-}$ mice were healthy and showed no changes in physical characteristics (body weight, or appearance of fur and whiskers) at 3 months old (Fig 1C). Although Luvisetto et al. (2008) have recently reported that Cyp $D^{-/-}$ mice show adult onset obesity, our mice did not show gross changes in physical characteristics, including body weight, with age (data not shown).

Histological appearance of the hippocampus in Cyp $D^{-/-}$ mice

Strong immunoreactivity for Cyp D was observed in the granule cell layer and pyramidal cell layer in the hippocampus (Fig. 1D). High magnification, Cyp D immunoreactivity in the CA1 regions merged with immunoreactivity to NeuN, a neuronal marker (Fig. 1E). With enhanced sensitivity of microscopy, Cyp D immunoreactivity was also observed in astrocytes, though sparsely (Fig. 1E). No Cyp D protein was pressed in the brains of Cyp $D^{-/-}$ mice as confirmed by immunofluorescent staining (Fig. 1D). Nissl staining and immunostaining for the astrocyte marker GFAP showed neither gross structural abnormalities (Fig. 1D) nor any morphological abnormality of neuronal cells and astrocytes (Fig. 1F). The expression levels of the dendritic marker MAP2, neuronal growth cone marker GAP-43, presynaptic marker synaptophysin, and GFAP remained unchanged in hippocampal homogenates from Cyp $D^{-/-}$ mice as compared with those from wild-type mice (Fig. 1G; n= 10 per group; Student t-test).

A deficiency of Cyclophilin D inhibits the release of glutamate and acetylcholine in

the hippocampus

The release of neurotransmitters in the hippocampus plays an important role in learning and memory (Stefani and Gold, 2001; Mereu et al., 2003). Therefore, changes in the amounts of glutamate and acetylcholine released in the hippocampus were investigated by microdialysis in the Cyp $D^{-/-}$ mice. The basal levels of glutamate in the hippocampus of the wild-type and Cyp $D^{-/-}$ mice were 0.55 ± 0.13 and 0.46 ± 0.21 pmol/10 μl/10 min, respectively (mean± s.e.m.; n= 6-7 per group). The amount of glutamate released in response to high potassium (50 mM) in the hippocampus was significantly lower in the Cyp $D^{-/-}$ mice than in the wild-type mice (Fig. 2A; repeated ANOVA, post hoc Bonferroni/Dunn multiple range-test, $p< 0.05$). The basal levels of acetylcholine in the hippocampus of the wild-type and Cyp $D^{-/-}$ mice were 0.15 ± 0.04 and 0.17 ± 0.03 nmol/10 μl/10 min, respectively (mean± s.e.m.; n= 10-11 per group). The amount of acetylcholine released in response to high potassium (50 mM) in the hippocampus was significantly lower in the Cyp $D^{-/-}$ mice than in the wild-type mice (Fig. 2B; $p< 0.05$). These results indicate that a deficiency of Cyp D results in inhibition of the potassium-induced release of glutamate and acetylcholine in the hippocampus.

No influence of the Cyclophilin D deficiency on glutamatergic and cholinergic nervous system-related protein expression in the hippocampus

As demonstrated above, Cyp $D^{-/-}$ mice showed a hypoglutamatergic and hypocholinergic response in the hippocampus in the presence of high potassium. It was possible that the deficiency in Cyp D affected the expression of these neuronal system-related proteins such as receptors, synthetases, degradation enzymes and

transporters. To test this possibility, the expression of NMDA receptor subunits, glutaminase (GLS), glutamate transporters, choline acetyltransferase (ChAT), and acetyltransferase (AChE) was analyzed by Western blotting. There was no significant difference in NR1, NR2A, NR2B, GLS, GLAST, GLT-1, ChAT and AChE protein levels in the hippocampus between wild-type and Cyp $D^{-/-}$ mice (Fig. 3; n= 10 per group; Student t-test). These data results that the hypoglutamatergic and hypocholinergic response observed in Cyp $D^{-/-}$ mice was not due to changes in expression levels of proteins involved in these neurotransmitters response.

Impairment by Cyclophilin D deficiency of learning and memory

Spontaneous alternation in the Y-maze test: We evaluated short-term memory using a Y-maze test. There was no significant difference in the number of arm entries between the two groups (Fig. 4A; n= 16-17 per group; Student t-test), suggesting that all mice have the same levels of motivation, curiosity, and motor function. However, Cyp $D^{-/-}$ mice showed significantly reduced spontaneous alternation behavior in the Y-maze compared with wild-type mice (Fig. 4B; $p< 0.05$), indicating an impairment of short-term memory.

Object recognition in the novel-object recognition test: We evaluated the visual recognition memory of Cyp $D^{-/-}$ mice using the novel-object recognition test. During the training session, there were no significant differences in exploratory preference between the two objects (Fig. 5A; n= 16-17 per group; repeated ANOVA, post hoc Bonferroni/Dunn multiple range-test) and the total time spent exploring both objects between the two groups (Fig.5B), suggesting that all mice have the same levels of

motivation, curiosity, and interest in exploring novel objects.

For the retention session, both groups of mice took longer to explore the novel object than the familiar object (Fig. 5A, $p< 0.01$). However, the level of exploratory preference for the novel objects was significantly decreased in Cyp $D^{-/-}$ mice compared to wild-type mice (Fig. 5A, $p< 0.01$), indicating an impairment of visual recognition memory.

Reference memory in the Morris water maze test: We evaluated reference memory using the Morris water maze test. Both groups of mice managed to learn the position of the hidden platform (Fig. 6A). However, Cyp $D^{-/-}$ mice took significantly longer time and distance to reach the platform than wild-type mice (Fig. 6A; n= 16-17 per group; repeated ANOVA, post hoc Bonferroni/Dunn multiple range-test; $p< 0.01$), indicating an impairment of reference memory. When the probe test was carried out following the tenth block of training, wild-type mice searched preferentially in the trained quadrant (Fig. 6B; repeated ANOVA, post hoc Bonferroni/Dunn multiple range-test; $p< 0.01$) but Cyp $D^{-/-}$ mice did not. The decreased ability did not reflect a loss of swimming ability and motivation because swimming speed and distance in the probe test were similar to those in wild-type mice (swimming speed; wild-type mice: 19.14 ± 0.78 cm/ sec, Cyp D-/- mice: 16.12 ± 1.33 cm/ sec, swimming distance; wild-type mice: 1141 ± 47 cm, Cyp D-/- mice: 962 ± 80 cm).

Associative learning in the cued and contextual fear conditioning tests: We evaluated associative learning in the conditioned fear learning test. In the preconditioning phase, the mice of both groups hardly showed any freezing response,

and there were no differences in basal levels of the freezing response between the groups (Fig. 7A, B; n= 16-17 per group; repeated ANOVA, post hoc Bonferroni/Dunn multiple range-test). In the contextual learning test, both groups showed a marked contextual freezing response 24 h after fear conditioning (Fig. 7A; $p< 0.01$). However, Cyp $D^{-/-}$ mice exhibited less of a freezing response in the contextual tests (Fig. 7A; $p< 0.01$), indicating an impairment of associative learning. In the cued learning test, Cyp $D^{-/-}$ mice exhibited less freezing (Fig. 7B; $p< 0.01$), indicating an impairment of associative learning. Furthermore, no aberrant nociceptive responses to electric footshocks were observed in the Cyp $D^{-/-}$ mice: the footshock thresholds in the Cyp $D^{-/-}$ mice (flinching, 0.28 ± 0.02 mA; vocalizing, 0.62 ± 0.05 mA; jumping, 0.78 ± 0.08 mA) were the same as those in wild-type mice (flinching, 0.22 ± 0.03 mA; vocalizing, 0.77 ± 0.05 mA; jumping, 0.71 ± 0.11 mA).

Recapitulation of cyclophilin D deficiency by infusion of cyclosporine A into the hippocampus

To examine the role of hippocampal Cyp D in learning and memory, we microinjected CsA, an inhibitor of Cyp D, into the hippocampus, and evaluated its effect on performance in the novel-object recognition test and conditioned fear learning test. In the novel-object recognition test, the mice were microinjected with CsA (100 pmol/mouse/unilateral) 10 min before the training trial. During the training session, there were no significant differences in exploratory preference between the two objects and total exploratory time between the two groups (Fig. 8A, B; n= 8-9 per group; repeated ANOVA, post hoc Bonferroni/Dunn multiple range-test). However, the level of exploratory preference for the novel objects in mice treated with CsA was

significantly decreased compared to that in mice treated with vehicle (Fig. 8A, $p< 0.05$), indicating a role for hippocampal Cyp D in this form of learning and memory. In the conditioned fear learning test, CsA was microinjected into the hippocampus 10 min before the conditioning trial. The mice treated with CsA exhibited less of a freezing response 24 h after fear conditioning in the contextual tests, which is known to be hippocampus-dependent (Fig. 8C; n= 16-17 per group; Student t-test; $p< 0.01$). But, there was no difference in the cued freezing response 24 h after fear conditioning among the groups in the cued learning test, which is known to be hippocampus-independent (Fig. 8D). These results indicate that hippocampal Cyp D plays a role in the hippocampal-dependent form of learning and memory.

Discussion

In this study, we analyzed mice with a deficiency of Cyp D to define its role in cognitive functions. Our behavioral data showed that Cyp $D^{-/-}$ mice have subtle but significant impairments of short-term memory in the Y-maze test, visual recognition memory in the novel-object recognition test, reference memory in the water maze test, and associative learning in the conditioned fear learning test. It is unlikely that the impaired performance of Cyp $D^{-/-}$ mice in learning and memory tests is due to changes in motivation or sensorimotor function, since the motivation for each of these behavioral tests is different, and different skills are required for a good performance in each test. Actually, there were no differences in total arm entries in the Y-maze test, total time spent exploring objects in the novel object test, swimming speed in the Morris water maze test, and freezing response in the preconditioning phase and nociceptive response between the wild-type and Cyp $D^{-/-}$ mice.

Cyp D immunoreactivity is abundant in neuronal layers but sparse in astrocytes in the adult mouse brain. Naga et al. (2007) also showed that Cyp D is present at high levels in neurons and low levels in astrocytes in adult rat brain using immunohistochemistry and in primary rat neuron and astrocyte cultures using Western blotting. Although it is possible that Cyp D deficiency-induced developmental abnormalities in the neuronal and astrocytic architecture lead to cognitive dysfunctions, we did not observe histopathological abnormalities on Nissl staining and GFAP immunostaining or the irregular expression of neuronal (MAP2a-c, GAP-43 and synaptophysin) and glial (GFAP) marker proteins on Western blotting. Hippocampus as well as perirhinal and prefrontal cortex is crucial for recognition memory in the novel-object recognition test (Rampon et al., 2000; Winters and Bussey., 2005; Nagai et

al., 2007). Reference memory in the Morris water maze test (Morris et al., 1982) and associative learning in the contextual, but not cued conditioned fear learning test (Phillips and LeDoux, 1992), are dependent on the hippocampus. Hippocampal infusion of CsA, an inhibitor of Cyp D (Halestrap and Davidson, 1990), replicated the hippocampus-dependent behavioral cognitive dysfunctions (impairments of recognition memory in the novel-object recognition test and of associative learning in the contextual test) observed in Cyp $D^{-/-}$ mice, except for the impairment of associative learning in the cued conditioned fear learning test, which is known to depend on the amygdala (Phillips and LeDoux, 1992). Taken together, these results strongly indicate that the role of Cyp D in cognitive functions is functional rather than developmental in nature.

Mitochondrial calcium buffering is an important regulator of synaptic function (Billups and Forsythe, 2002; Tang and Zucker, 1997). Recent studies have suggested that Cyp D-regulated MPT plays an important role in mitochondrial synaptic Ca^{2+} buffering, hippocampal synaptic plasticity, and learning and memory (Weeber et al., 2002; Levy et al., 2003; Naga et al., 2007). Mitochondria from synaptosomes, isolated from rat cerebral cortex, have less Ca^{2+} buffering ability than the nonsynaptic pool of mitochondria (Brown et al., 2006). This difference reflects the higher levels of Cyp D in synaptic than nonsynaptic mitochondria (Naga et al., 2007). The application of CsA, a deficiency of Cyp D, and a deficiency of VDAC all increase Ca^{2+} uptake capacity in isolated mitochondria (Levy et al., 2003; Naga et al., 2007). Interestingly, the application of CsA and a deficiency of VDAC impair paired-pulse facilitation and long-term potentiation (Weeber et al., 2002; Levy et al., 2003). The phenomena of paired pulse facilitation are generally accepted as a model of the presynaptic component of synaptic plasticity (Gottschalk et al., 1998). These results suggest that the cognitive

dysfunction and impaired neurotransmission observed in Cyp $D^{-/-}$ mice is ascribable to deficiency of Cyp D-dependent MPT.

Excitatory transmitters such as acetylcholine and glutamate change neural information processing by regulating the release of synaptic transmitters and modifying long-term synaptic plasticity (Giocomo and Hasselmo, 2007). In addition, the release of glutamate and acetylcholine in hippocampus is related to cognitive performance in behavioral tests (Stefani and Gold, 2001; Mereu et al., 2003). In the present study, Cyp $D^{-/-}$ mice had lower extracellular glutamate and acetylcholine levels in response to high potassium in the hippocampus than did the wild-type mice. Previously, a decrease in spontaneous extracellular glutamate release and increase in levels of the glutamate transporter GLAST were observed in schizophrenic animal models, which show impairments of memory (Murai et al., 2007; Mouri et al., 2007b). It is unlikely that the deficient in glutamate and acetylcholine transmission in Cyp $D^{-/-}$ mice is due to alternation of neurotransmitter synthesis, metabolism and uptake, because there was no difference in the protein expressions of GLS, GLAST or GLT-1 between wild-type and Cyp $D^{-/-}$ mice. Although we have no detail data about neurotransmitter levels in response to other potassium concentration, activities of neurotransmitters enzymes and transporters in Cyp $D^{-/-}$ and hippocampal CsA-infused mice, our results along with other recent findings suggest that Cyp D and MPT play important roles in synaptic transmission.

Luvisetto et al. (2008) have reported that the Cyp $D^{-/-}$ mice generated by Basso et al. (2005) show adult onset obesity, increased anxiety/emotionality in the open field test and elevated plus maze test, and a facilitation of learning in the active and passive avoidance test at 10 months old. As far as the obesity is concerned, we did not observe a significant

difference in the body weight of Cyp $D^{-/-}$ mice up to 40 months, as compared with control littermates. We do not know the reason for this difference. Although our results are consistent with some of the results described by Luvisetto et al. (2008), notably that Cyp $D^{-/-}$ mice exhibited increased anxiety/emotionality in the elevated plus maze test (unpublished data), we did not observe any facilitation of learning and memory in our Cyp $D^{-/-}$ mice. It is conceivable that the avoidance behavior of Cyp $D^{-/-}$ mice is due to greater anxiety rather than greater learning ability. Du et al. (2008) have reported that the Cyp $D^{-/-}$ mice generated by Bains et al. (2005) show normal synaptic plasticity and spatial memory in radial water maze test. These differences between Du's and our data might be due to different behavioral test, because the $CypD^{-/-}$ mice shows normal but slightly increase of error in the behavior test at 6 months old and decrease of long term potentiation at 12-13 moths old (Du et al. 2008). More extensive investigation will be necessary to clarify these differences.

In summary, mice lacking Cyp D display cognitive dysfunction probably caused by the hypofunction of neurotransmission without developmental abnormalities. In pathological process, blockade of Cyp D could be a potent therapeutic strategy for degenerative disorders such as Alzheimer's disease, ischemia and multiple sclerosis. It is possible that blockade of Cyp D impairs rather than facilitates cognitive function in normal condition. Our findings could contribute understanding not only the physiological roles of Cyp D in cognition but also appropriate use of Cyp D blocker for degenerative disorders.

Hippocampus

References

Baines CP, Kaiser RA, Purcell NH, Blair NS, Osinska H, Hambleton MA, Brunskill EW, Sayen MR, Gottlieb RA, Dorn GW, Robbins J, Molkentin JD. 2005. Loss of cyclophilin D reveals a critical role for mitochondrial permeability transition in cell death. *Nature* 434: 658-662.

Basso E, Fante L, Fowlkes J, Petronilli V, Forte MA, Bernardi P. 2005. Properties of the permeability transition pore in mitochondria devoid of Cyclophilin D. *J Biol Chem* 280: 18558-18561.

Bernardi P. 1999. Mitochondrial transport of cations: channels, exchangers, and permeability transition. *Physiol Rev* 79: 1127-1155.

Billups B, Forsythe ID. 2002. Presynaptic mitochondrial calcium sequestration influences transmission at mammalian central synapses. *J Neurosci* 22: 5840-5847

Brown MR, Sullivan PG, Geddes JW. 2006. Synaptic mitochondria are more susceptible to Ca2+overload than nonsynaptic mitochondria. *J Biol Chem* 281: 11658-11668.

Crompton M, Virji S, Ward JM. 1998. Cyclophilin-D binds strongly to complexes of the voltage-dependent anion channel and the adenine nucleotide translocase to form the permeability transition pore. *Eur J Biochem* 258: 729-735

Dodge FA Jr, Rahamimoff R. 1967. Co-operative action a calcium ions in transmitter release at the neuromuscular junction. *J Physiol* 193: 419-432.

Du H, Guo L, Fang F, Chen D, Sosunov AA, McKhann GM, Yan Y, Wang C, Zhang H, Molkentin JD, Gunn-Moore FJ, Vonsattel JP, Arancio O, Chen JX, Yan SD. 2008. Cyclophilin D deficiency attenuates mitochondrial and neuronal perturbation and ameliorates learning and memory in Alzheimer's disease. *Nat Med.* 14: 1097-1105

Galat A. Peptidylproline cis-trans-isomerases: immunophilins. 1993. *Eur J Biochem.* 216: 689-707.

Giocomo LM, Hasselmo ME. 2007. Neuromodulation by glutamate and acetylcholine can change circuit dynamics by regulating the relative influence of afferent input and

John Wiley & Sons

excitatory feedback. *Mol Neurobiol* 36: 184-200.

Gottschalk W, Pozzo-Miller LD, Figurov A, Lu B. 1998. Presynaptic modulation of synaptic transmission and plasticity by brain-derived neurotrophic factor in the developing hippocampus. *J Neurosci* 18: 6830-6839.

Halestrap AP, McStay GP, Clarke SJ. 2002. The permeability transition pore complex: another view. *Biochimie* 84: 153-166.

Halestrap AP, Davidson AM. 1990. Inhibition of Ca2(+)-induced large-amplitude swelling of liver and heart mitochondria by cyclosporin is probably caused by the inhibitor binding to mitochondrial-matrix peptidyl-prolyl cis-trans isomerase and preventing it interacting with the adenine nucleotide translocase. *Biochem J* 268: 153-160.

Kang JS, Tian JH, Pan PY, Zald P, Li C, Deng C, Sheng ZH. 2008. Docking of axonal mitochondria by syntaphilin controls their mobility and affects short-term facilitation. *Cell* 132: 137-148.

Kokoszka JE, Waymire KG, Levy SE, Sligh JE, Cai J, Jones DP, MacGregor GR, Wallace DC. 2004. The ADP/ATP translocator is not essential for the mitochondrial permeability transition pore. *Nature* 427: 461-465.

Lee D, Lee KH, Ho WK, Lee SH. 2007. Target cell-specific involvement of presynaptic mitochondria in post-tetanic potentiation at hippocampal mossy fiber synapses. *J. Neurosci* 27: 13603-13613.

Leung AW, Halestrap AP. 2008. Recent progress in elucidating the molecular mechanism of the mitochondrial permeability transition pore. *Biochim Biophys Acta* 1777: 946-952.

Levy M, Faas GC, Saggau P, Craigen WJ, Sweatt JD. 2003. Mitochondrial regulation of synaptic plasticity in the hippocampus. *J Biol Chem* 278: 17727-17734.

Luvisetto S, Basso E, Petronilli V, Bernardi P, Forte M. 2008. Enhancement of anxiety, facilitation of avoidance behavior, and occurrence of adult-onset obesity in mice lacking mitochondrial cyclophilin D. *Neuroscience* In press

Long AA, Kim E, Leung HT, Woodruff E 3rd, An L, Doerge RW, Pak WL, Broadie K. 2008. Presynaptic calcium channel localization and calcium-dependent synaptic vesicle exocytosis regulated by the Fuseless protein. *J Neurosci* 28: 3668-3682.

Matsumoto S, Friberg H, Ferrand-Drake M, Wieloch T. 1999. Blockade of the mitochondrial permeability transition pore diminishes infarct size in the rat after transient middle cerebral artery occlusion. *J Cereb Blood Flow Metab* 19: 736-741.

Mereu G, Fà M, Ferraro L, Cagiano R, Antonelli T, Tattoli M, Ghiglieri V, Tanganelli S, Gessa GL, Cuomo V. 2003. Prenatal exposure to a cannabinoid agonist produces memory deficits linked to dysfunction in hippocampal long-term potentiation and glutamate release. *Proc Natl Acad Sci U S A* 100: 4915-4920

Morris RG, Garrud P, Rawlins JN, O'Keefe J. 1982. Place navigation impaired in rats with hippocampal lesions. *Nature* 297: 681-683.

Morris RL, Hollenbeck PJ. 1993. The regulation of bidirectional mitochondrial transport is coordinated with axonal outgrowth. *J Cell Sci* 104: 917-927.

Mouri A, Noda Y, Hara H, Mizoguchi H, Tabira T, Nabeshima T. 2007a. Oral vaccination with a viral vector containing Abeta cDNA attenuates age-related Abeta accumulation and memory deficits without causing inflammation in a mouse Alzheimer model. *FASEB J* 21: 2135-2148.

Mouri A, Noda Y, Noda A, Nakamura T, Tokura T, Yura Y, Nitta A, Furukawa H, Nabeshima T. 2007b. Involvement of a dysfunctional dopamine-D1/N-methyl-d-aspartate-NR1 and Ca2+/calmodulin-dependent protein kinase II pathway in the impairment of latent learning in a model of schizophrenia induced by phencyclidine. *Mol Pharmacol* 71: 1598-1609.

Murai R, Noda Y, Matsui K, Kamei H, Mouri A, Matsuba K, Nitta A, Furukawa H, Nabeshima T. 2007 Hypofunctional glutamatergic neurotransmission in the prefrontal cortex is involved in the emotional deficit induced by repeated treatment with phencyclidine in mice: implications for abnormalities of glutamate release and NMDA-CaMKII signaling. *Behav Brain Res* 180: 152-160.

Muramatsu Y, Furuichi Y, Tojo N, Moriguchi A, Maemoto T, Nakada H, Hino M, Matsuoka N. 2007 Neuroprotective efficacy of FR901459, a novel derivative of cyclosporin A, in in vitro mitochondrial damage and in vivo transient cerebral ischemia models. *Brain Res.* 1149: 181-190.

Naga KK, Sullivan PG, Geddes JW. 2007. High cyclophilin D content of synaptic mitochondria results in increased vulnerability to permeability transition. *J Neurosci* 27: 7469-7475.

Nagai T, Takuma K, Kamei H, Ito Y, Nakamichi N, Ibi D, Nakanishi Y, Murai M, Mizoguchi H, Nabeshima T, Yamada K. 2007. Dopamine D1 receptors regulate protein synthesis-dependent long-term recognition memory via extracellular signal-regulated kinase 1/2 in the prefrontal cortex. *Learn Mem* 14: 117-125.

Nakagawa T, Shimizu S, Watanabe T, Yamaguchi O, Otsu K, Yamagata H, Inohara H, Kubo T, Tsujimoto Y. 2005. Cyclophilin D-dependent mitochondrial permeability transition regulates some necrotic but not apoptotic cell death. *Nature* 434: 652-658.

Nicholls DG, Budd SL. 2000. Mitochondria and neuronal survival. *Physiol Rev* 80: 315-360.

Norenberg MD, Rao KV. 2007. The mitochondrial permeability transition in neurologic disease. *Neurochem Int.* 50: 983-997.

Paxinos G, Franklin KBJ. 2004. The mouse Brain in Stereotaxic Coordinates, Compact 2nd edition, Elsevier Academic Press: San Diego.

Phillips RG., LeDoux JE. 1992. Differential contribution of amygdala and hippocampus to cued and contextual fear conditioning. Behav Neurosci 106: 274-285.

Rampon C, Tang YP, Goodhouse J, Shimizu E, Kyin M, Tsien JZ. 2000. Enrichment induces structural changes and recovery from nonspatial memory deficits in CA1 NMDAR1-knockout mice. *Nat Neurosci* 3: 238-244.

Rowland KC, Irby NK, Spirou GA. 2000. Specialized synapse-associated structures within the calyx of Held. *J Neurosci* 20: 9135-9144.

Schinzel AC, Takeuchi O, Huang Z, Fisher JK, Zhou Z, Rubens J, Hetz C, Danial NN, Moskowitz MA, Korsmeyer SJ. 2005. Cyclophilin D is a component of mitochondrial permeability transition and mediates neuronal cell death after focal cerebral ischemia. *Proc Natl Acad Sci U S A* 102: 12005-12010.

Shepherd GM, Harris KM. 1998. Three-dimensional structure and composition of CA3-->CA1 axons in rat hippocampal slices: implications for presynaptic connectivity and compartmentalization. *J Neurosci* 18: 8300-8310.

Stefani MR, Gold PE. 2001. Intrahippocampal infusions of k-atp channel modulators influence spontaneous alternation performance: relationships to acetylcholine release in the hippocampus. *J Neurosci* 21: 609-614.

Tang Y, Zucker RS. 1997. Mitochondrial involvement in post-tetanic potentiation of synaptic transmission. *Neuron* 118: 483-491

Weeber EJ, Levy M, Sampson MJ, Anflous K, Armstrong DL, Brown SE, Sweatt JD, Craigen WJ. 2002. The role of mitochondrial porins and the permeability transition pore in learning and synaptic plasticity. *J Biol Chem* 277: 18891-18897.

Winters BD, Bussey TJ. 2005. Glutamate receptors in perirhinal cortex mediate encoding, retrieval, and consolidation of object recognition memory. J Neurosci 25: 4243-4251.

Woodfield K, Rück A, Brdiczka D, Halestrap AP. 1998. Direct demonstration of a specific interaction between cyclophilin-D and the adenine nucleotide translocase confirms their role in the mitochondrial permeability transition. *Biochem J* 336: 287-290.

Zoratti M, Szabò I. 1995. The mitochondrial permeability transition. *Biochim Biophys Acta* 1241: 139-176.

Hippocampus

John Wiley & Sons

Acknowledgements

This study was supported in part by the Program for Promotion of Fundamental Studies in Health Sciences of the National Institute of Biomedical Innovation (NIBIO05-27), by the Academic Frontier Project for Private Universities (2007-2011) from the Ministry of Education, Culture, Sports, Science and Technology of Japan, by an International Research Project supported by The Meijo Asian Research Center (MARC), by a Grant-in-aid for Exploratory Research from Japan Society for the Promotion of Science (JSPS), by a Grant-in-aid for Scientific Research (B) from JSPS, by a Grant-in-aid on Priority Areas from JSPS, by Health and Labour Sciences Research Grant for Research on Regulatory Science of Pharmaceuticals and Medical Devices from the Ministry of Health, Labour and Welfare, Japan, by a Grant from the INSERM-JSPS Joint Research Project from JSPS, by Solution Oriented Research for Science and Technology (SORST) of the Japan Science and Technology Agency (JST), and by a Grant-in-aid for Creative Scientific Research from JSPS.

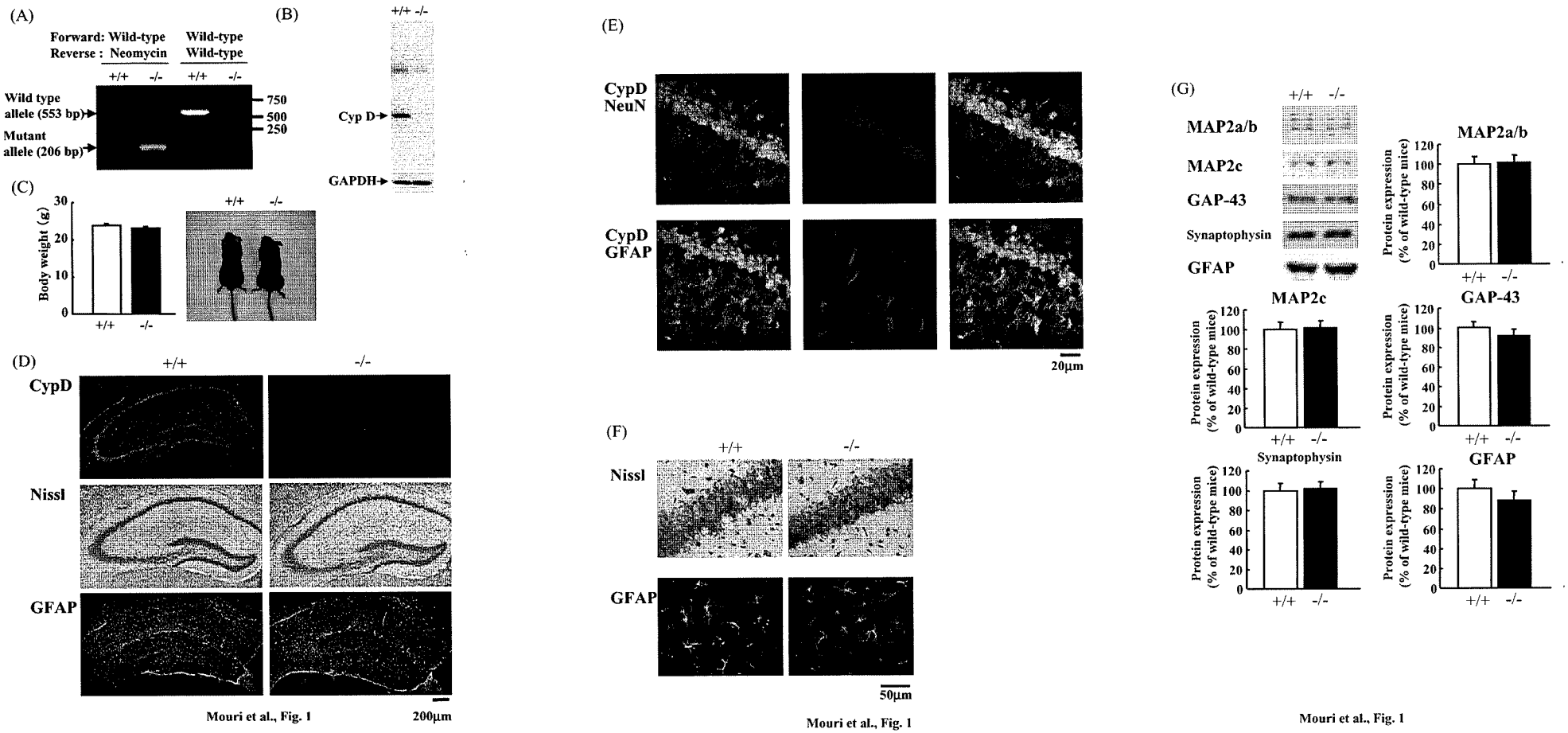

Fig. 1: Histological characterization of Cyclophilin D and of Cyclophilin D-deficient mice.

(A): Determination of genotype: Genotyping was performed by PCR and gel electrophoresis. The wild-type allele (553 bp) and mutant allele (206 bp) were identified by PCR using wild-type forward and reverse primers and the wild-type forward primer and neomycin-specific reverse primer, respectively. (B): Protein expression of Cyp D in Cyp D-/- mice: Protein extracts from the whole brain of Cyp $D^{-/-}$ and wild type mice were examined by Western blotting. (C): Representative examples of wild-type and Cyp $D^{-/-}$ mice at 3 month olds: Body weights of wild-type and Cyp $D^{-/-}$ mice were 23.9 ± 0.44 and 23.0 ± 0.65 g, respectively. (D): Cyp D-, GFAP-immunostaining, and Nissl staining in the Cyp $D^{-/-}$ and wild-type mice: Slices of Hippocampus obtained from Cyp $D^{-/-}$ mice showed no immunoreactivity to anti-Cyp D antibody and no abnormal structure or glial distribution. (E): Localization of Cyp D in the hippocampus: Confocal immunofluorescent images obtained from coronal sections from wild-type mice. Cyp D immunoreactivity was evident in neuronal cell layers in CA1 and localized to cells positive for NeuN, a marker of neuronal cells. Enhanced sensitivity revealed Cyp D immunoreactivity in cells positive for GFAP, a marker of astrocytes. (F): A higher magnitude image of the hippocampal CA1 region. There was no morphological change to neuronal cells and astrocytes in Cyp $D^{-/-}$ mice. (G): Western blotting of homogenates from the hippocampus for proteins described. No difference was observed between the two genotypes (wild-type mice, n= 10; Cyp $D^{-/-}$ mice, n= 10; Student t-test). +/+: wild-type mice, -/-: Cyp $D^{-/-}$ mice.

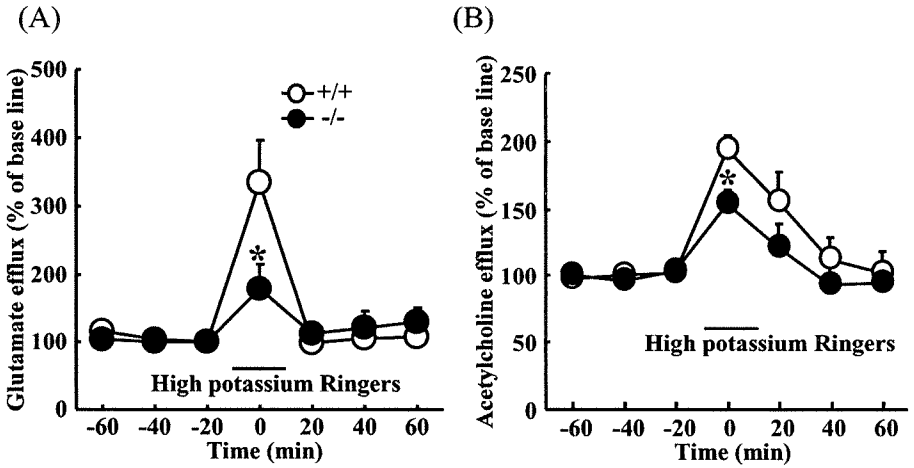

Mouri et al., Fig. 2

Fig. 2: Deficiency of Cyclophilin D inhibits the release of glutamate and acetylcholine in the hippocampus.

High potassium-evoked release of glutamate (A) and acetylcholine (B) from the hippocampus in the Cyp $D^{-/-}$ and wild type mice; High potassium-induced release of glutamate from the hippocampus was measured in the Cyp $D^{-/-}$ and wild-type mice. Values correspond to the mean ± s.e.m. (wild-type mice, n= 6; Cyp $D^{-/-}$ mice, n= 7). Results with repeated ANOVA were: time: $F(3,33)= 11.36$, $p< 0.01$, Cyp D deficiency: $F(1,33)= 2.28$, $p= 0.16$, interaction time with Cyp D deficiency: $F(3,33)= 4.48$, $p< 0.01$. High potassium-induced release of acetylcholine from the hippocampus was measured in the Cyp $D^{-/-}$ mice. Values correspond to the mean ± s.e.m. (wild-type mice, n= 10; Cyp $D^{-/-}$ mice; n= 11). Results with repeated ANOVA were: time: $F(3,57)= 11.54$, $p< 0.01$, Cyp D deficiency: $F(1,57)= 2.16$, $p= 0.16$, interaction of time with Cyp D deficiency: $F(3,57)= 0.45$, $p= 0.71$, *$p< 0.05$ vs wild-type mice. +/+: wild-type mice, -/-: Cyp $D^{-/-}$ mice.

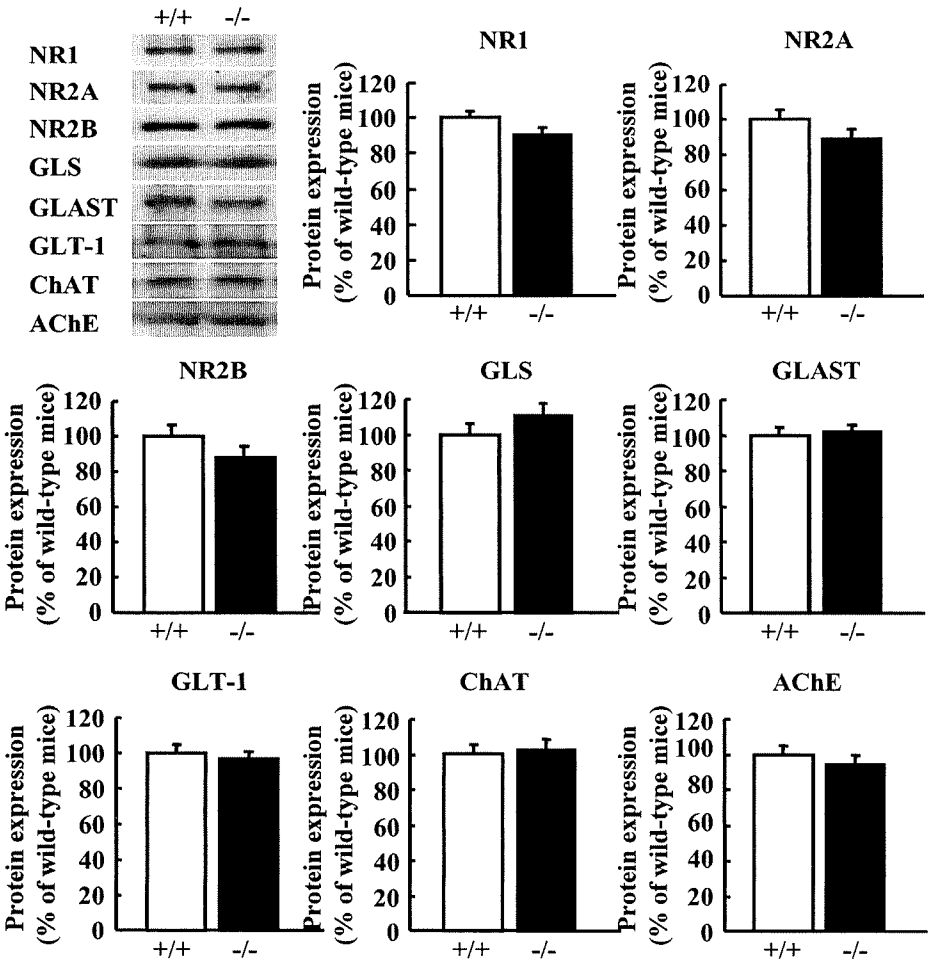

Mouri et al., Fig. 3

Fig. 3: No influence of Cyclophilin D deficiency on glutamatergic nervous system-related protein expression in the hippocampus.

Western blot analysis of homogenates from the hippocampus of the Cyp $D^{-/-}$ and wild-type mice. No difference was observed between the two genotypes (wild-type mice, n= 10; Cyp $D^{-/-}$ mice, n= 10; Student t-test). NR1: NMDA receptor 1 subunit, NR2A: NMDA receptor 2A subunit, NR2B: NMDA receptor 2B subunit, GLS: glutaminase, GLAST: glutamate-aspartate transporter, GLT-1: glial glutamate transporter-1, ChAT: choline acetyltrasferase, AChE: Aetylcholinesterase. +/+: wild-type mice, -/-: Cyp $D^{-/-}$ mice.

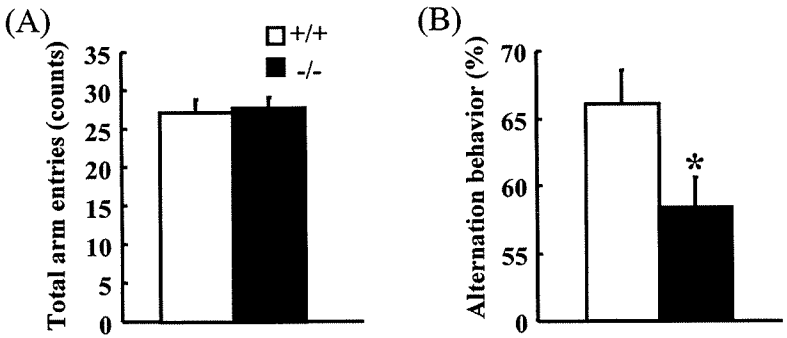

Mouri et al., Fig. 4

Fig. 4: Impairment of short-term memory by Cyclophylin D deficiency in the Y-maze test.

(A): Total arm entries, (B): Alternation behavior. Percent alternation during an 8-min session in the Y-maze test was measured. Values indicate the mean± s.e.m. (wild-type mice, n= 17; Cyp D$^{-/-}$ mice; n= 16). *p< 0.05 vs wild-type mice (Student t-test). +/+: wild-type mice, -/-: Cyp D$^{-/-}$ mice.

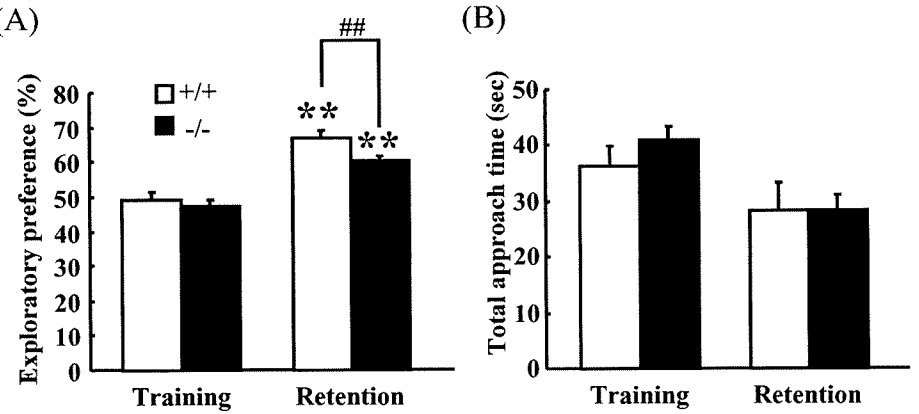

Mouri et al., Fig. 5

Fig. 5: Impairment of object recognition memory by Cyclophylin D deficiency in the novel-object recognition test.

(A): Exploratory preference, (B): Total approach time. The retention session was carried out 24 h after the training. Exploratory preference during a 10-min session in the novel-object recognition test was measured. Values indicate the mean± s.e.m. (wild-type mice, n= 17; Cyp D$^{-/-}$ mice; n= 16). Results with the repeated ANOVA were: exploratory preference: training/retention: $F(1,31)= 122.53$, $p< 0.01$, Cyp D deficiency: $F(1,31)= 9.52$, $p< 0.01$, interaction of training/retention with Cyp D deficiency: $F(1,31)= 2.22$, $p= 0.14$, total approach time: training/retention: $F(1,31)= 28.32$, $p< 0.01$, Cyp D deficiency: $F(1,31)= 0.62$, $p= 0.44$, interaction of training/retention with Cyp D deficiency: $F(1,31)= 1.10$, $p= 0.30$, **p< 0.01 vs training, ##p< 0.01 vs trained, wild-type mice. +/+: wild-type mice, -/-: Cyp D$^{-/-}$ mice.

(A) Reference memory test

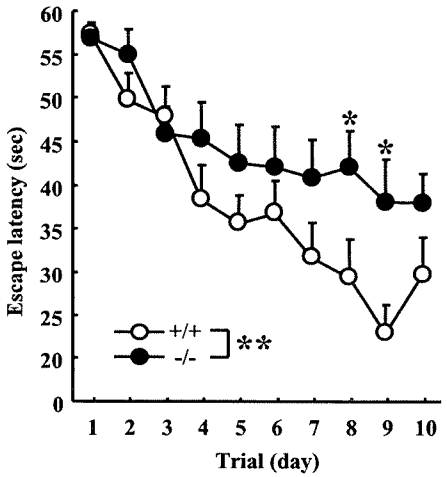

(B) Probe test

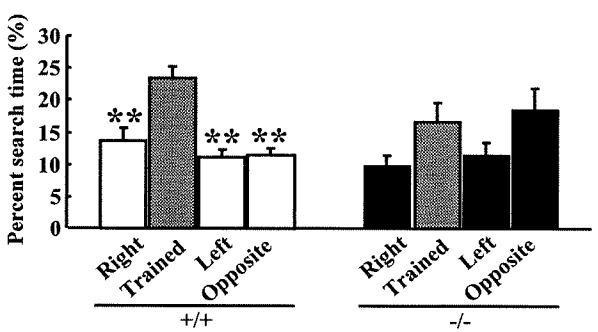

Mouri et al., Fig. 6

Fig. 6: Impairment of reference memory by Cyclophylin D deficiency in the Morris water maze test.

(A): Reference memory test. Escape latency during a 60-sec session in the water maze test was measured. Values indicate the mean± s.e.m. (wild-type mice, n= 17; Cyp $D^{-/-}$ mice; n= 16). Results with the repeated ANOVA were: trial: $F(9,279)= 11.96$, $p< 0.01$, animal group: $F(1,31)= 7.27$, $p< 0.05$, interaction of trial with animal group: $F(9,279)= 1.13$, $p= 0.34$. **p< 0.01, *p< 0.05 vs wild-type mice. (B): Probe test. The probe test was performed after training on day 10 in the Morris water maze test. Percent search time during a 60-sec session in the water maze test was measured. Values indicate the mean± s.e.m. (wild-type mice, n= 17; Cyp $D^{-/-}$ mice; n= 16). Results with the repeated ANOVA were: quadrant: $F(3,93)= 5.57$, $p< 0.01$, Cyp D deficiency: $F(1,31)= 0.01$, $p= 0.91$, interaction of quadrant with Cyp D deficiency: $F(3,93)= 2.95$, $p< 0.05$. **p< 0.01 vs trained quadrant. +/+: wild-type mice, -/-: Cyp $D^{-/-}$ mice.

(A) Contextual

(B) Cue

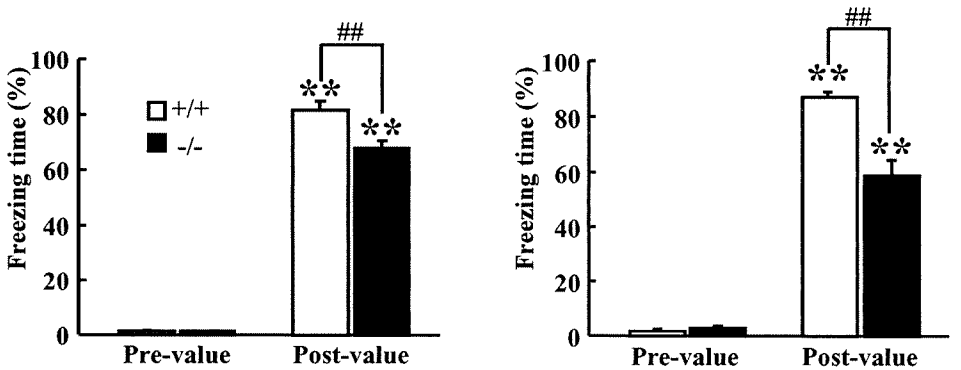

Mouri et al., Fig. 7

Fig. 7: Impairment of associative learning by Cyclophylin D deficiency in the conditioned-fear learning test.

The test session was carried out 24 h after the conditioning. Context-dependent (A) and Cue-dependent (B) freezing time was measured. Values indicate the mean± s.e.m. (wild-type mice, n= 17; Cyp $D^{-/-}$ mice; n= 16). Results with the repeated ANOVA were: context-dependent test: conditioning: $F(1,31)= 1127.89$, $p< 0.01$, Cyp D deficiency: $F(1,31)= 9.12$, $p< 0.01$, interaction of conditioning with Cyp D deficiency: $F(1,31)= 9.12$, $p< 0.01$, cue-dependent test: conditioning: $F(1,31)= 703.45$, $p< 0.01$, Cyp D deficiency: $F(1,31)= 17.14$, $p< 0.01$, interaction of conditioning with Cyp D deficiency: $F(1,31)= 29.96$, $p< 0.01$, **p< 0.01 vs pre-conditioning. ##p< 0.01 vs conditioned, wild-type mice. +/+: wild-type mice, -/-: Cyp $D^{-/-}$ mice.

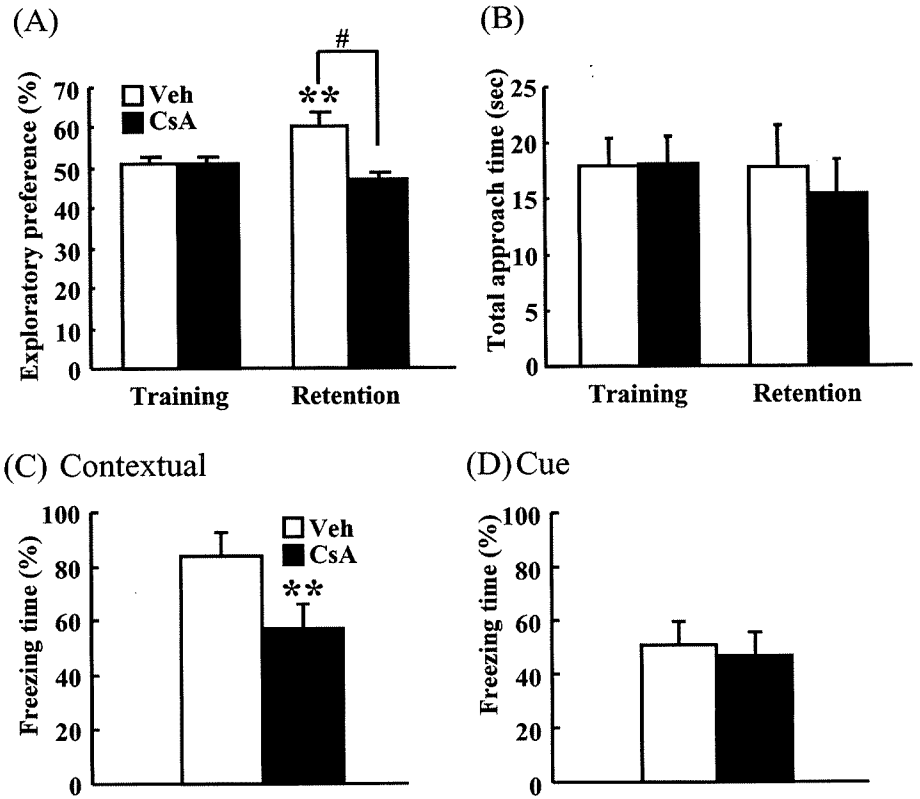

Mouri et al., Fig. 8

Fig. 8: Recapitulation of cyclophilin D deficiency by infusion of cyclosporine A into the hippocampus.

Novel object recognition test: (A): Exploratory preference, (B): Total approach time. The retention session was carried out 24 h after the training. Cyclosporine A (100 pmol/mouse/unilateral) was infused into the hippocampus 10 min before the training trial. Exploratory preference during a 10-min session in the novel-object recognition test was measured. Values indicate the mean± s.e.m. (vehicle-treated mice, n= 9; cyclosporine A-treated mice; n= 8). Results with the repeated ANOVA were: exploratory preference: training/retention: $F(1,15)= 2.67$, $p= 0.12$, treatment: $F(1,15)= 7.17$, $p< 0.05$, interaction training/retention with treatment: $F(1,15)= 12.83$, $p< 0.05$, total approach time: training/retention: $F(1,15)= 0.12$, $p= 0.64$, treatment: $F(1,15)= 0.06$, $p=0.81$, interaction training/retention with treatment: $F(1,15)= 0.89$, $p= 0.36$. **$p< 0.01$ vs training. #$p< 0.05$ vs trained, vehicle-treated mice. Conditioned-fear learning test: The test session was carried out 24h after the conditioning. Context-dependent (C) and cue-dependent (D) freezing time was measured. Values indicate the mean± s.e.m (vehicle-treated mice, n= 10; cyclosporine A-treated mice; n= 10). **$p< 0.01$ vs vehicle-treated mice (Student t-test). Veh: vehicle-treated mice, CsA: cyclosporine A-treated mice.

Journal of Pharmacological Sciences

Forum Minireview

Neuropsychotoxicity of Abused Drugs: Involvement of Matrix Metalloproteinase-2 and -9 and Tissue Inhibitor of Matrix Metalloproteinase-2 in Methamphetamine-Induced Behavioral Sensitization and Reward in Rodents

Hiroyuki Mizoguchi[1,2,3], Kiyofumi Yamada[1,2,*], and Toshitaka Nabeshima[1,4]

[1]*Department of Neuropsychopharmacology and Hospital Pharmacy, Nagoya University Graduate School of Medicine, Showa-ku, Nagoya 466-8560, Japan*
[2]*Laboratory of Neuropsychopharmacology, Division of Life Sciences, Graduate School of Natural Science & Technology, Kanazawa University, Kakuma-machi, Kanazawa 920-1192, Japan*
[3]*Futuristic Environmental Simulation Center, Research Institute of Environmental Medicine, Nagoya University, Furo-cho, Chikusa-ku, Nagoya 464-8601, Japan*
[4]*Department of Chemical Pharmacology, Meijo University Graduate School of Pharmaceutical Sciences, Nagoya 468-8503, Japan*

Received September 14, 2007; Accepted November 14, 2007

Abstract. Matrix metalloproteinases (MMPs) and their inhibitors (TIMPs) function to remodel the pericellular environment. We have investigated the role of the MMP/TIMP system in methamphetamine (METH) dependence in rodents, in which the remodeling of neural circuits may be crucial. Repeated METH treatment induced behavioral sensitization, which was accompanied by an increase in MMP-2/-9/TIMP-2 activity in the brain. An antisense TIMP-2 oligonucleotide enhanced the sensitization, which was associated with a potentiation of the METH-induced release of dopamine in the nucleus accumbens (NAc). MMP-2/-9 inhibitors blocked the METH-induced behavioral sensitization and conditioned place preference (CPP), a measure of the rewarding effect of a drug, and reduced the METH-increased dopamine release in the NAc. In MMP-2– and MMP-9–deficient mice, METH-induced behavioral sensitization and CPP as well as dopamine release were attenuated. The MMP/TIMP system may be involved in METH-induced sensitization and reward by regulating extracellular dopamine levels.

Keywords: abused drug, matrix metalloproteinase, tissue inhibitor of matrix metalloproteinase, methamphetamine, dopamine

Introduction

Drug dependence is a complex phenomenon with important psychological and social causes and consequences, which may be associated with neural plasticity and the remodeling of specific brain circuits caused by repeated exposure to drugs of abuse (1 – 3). Methamphetamine (METH), a common drug of abuse, has both acute and long-lasting effects on psychomotor behavior (4 – 6). These effects of METH are associated with an increase in extracellular dopamine levels in the brain, achieved by facilitating the release of dopamine from presynaptic nerve terminals and inhibiting its reuptake (7). It has been proposed that cellular and molecular mechanisms for drug dependence involve processes similar to those operating in other forms of synaptic plasticity such as learning and memory (1, 8). Although it has been demonstrated that repeated treatment with cocaine and amphetamine produces changes in neural morphology and synaptic connectivity in the mesolimbic system (9, 10), the mechanism underlying psychostimulant-induced remodeling of synaptic structures remains to be determined (11, 12).

*Corresponding author (affiliatinn #1).
kyamada@med.nagoya-u.ac.jp
Published online in J-STAGE
doi: 10.1254/jphs.FM0070139

In order to elucidate the mechanisms by which chronic drug exposure causes stable changes in the brain that may underlie the long-lasting behavioral abnormalities in dependent subjects, we compared the gene expression in the brains of rats that had previously received repeated morphine or METH treatment (12). We hypothesized that those genes whose expression was altered by repeated administration of morphine and METH could be candidates for drug-dependence–related genes. We used DNA microarray technology to profile the gene expression in the brains of drug-dependent animals. Since we hypothesized that the development of drug dependence is associated with activity-dependent synaptic plasticity and remodeling of the mesocorticolimbic dopaminergic system, we focused on the role of candidate genes found by the DNA microarray screening, especially in relation to cytokines/neurotrophic factor and extracellular matrix/proteases. As a result, we have demonstrated that tumor necrosis factor-α (TNF-α) (7, 11, 13), tissue plasminogen activator (tPA) (14 – 16), neuroglycan C (17), and matrix metalloproteinase (MMP) (18, 19) were involved in drug dependence.

In this review, we discuss a possible role for the /tissue inhibitor of MMP (TIMP) system in METH dependence.

MMP/TIMP system

MMPs function to remodel the pericellular environment, primarily through the cleavage of extracellular matrix (ECM) proteins (20). MMPs constitute a family of enzymes with more than 20 members identified to date, which require Zn^{2+} for their enzymatic activity. Several MMPs have a furin motif (MMP-11,-14, -15, -16, etc.) that allows for intracellular activation of the proteinase prior to its appearance on the outside of the cell, including all of the membrane-anchored members. Activation of the remaining MMPs requires extracellular proteolytic processing of the secreted zymogen into a fully active enzyme, which can be done by MMPs or some serine proteinases (21). Interestingly, the tPA/plasmin system is one of the regulators of MMP (22) and could play a pivotal role in degradation of the ECM (23). TNF-α can induce the expression of MMPs while MMPs also induce the activation and release of this cytokine.

MMP activity is regulated by interaction with TIMPs. TIMPs belong to a family of multifunctional secreted proteins (TIMP-1 – 4) and possess growth-promoting and cell cycle-regulating activities in various cell types (24). MMP and TIMP function to modulate functional and structural remodeling of the cellular architecture in the context of pathophysiology primarily through the cleavage of ECM proteins, bioavailability of growth factors and cytokines, and shedding of membrane receptors (20, 25). It has been recently demonstrated that neuronal TIMP-1 (26) and MMP-9 (27) are regulated by synaptic activity, suggesting that the balance between MMPs and TIMPs is important in the activity-dependent re-organization of the neuronal architecture with possible effects on synaptic physiology. Thus, the MMP/TIMP ratio and net MMP activity may be involved in brain development because extensive cellular migration and remodeling of the ECM are necessary for neural development (22, 28). A precise knowledge of the relative role of the major MMPs and TIMPs may be indispensable to delineate the mechanisms of brain development and remodeling as well as synaptic plasticity.

Changes in the expression of MMP-2, MMP-9, and TIMP-2 in the brain induced by METH

Gelatinases (MMP-2 and MMP-9) are capable of cleaving collagen IV and V, laminin, and chondroitin sulfate proteoglycan, which are associated with cell adhesion, and have been implicated specifically in cerebral ischemia (29), kainate-induced neuronal injuries (27), and hippocampal long-term potentiation (LTP) and memory (30). For example, MMP-2 plays a principal role in establishing the growth-promoting properties of denervated peripheral nerve (31). MMP-9, but not MMP-2, is particularly involved in dendritic remodeling in the hippocampus of adult rat (27).

We have demonstrated for the first time that repeated administration of METH leads to behavioral sensitization that is accompanied by the induction of MMP-2, MMP-9, and TIMP-2 expression in the brain including the frontal cortex (Fc) and nucleus acumbens (NAc) (Table 1) (18, 19). Our data also showed that MMP-2 and MMP-9 were expressed in neurons as well as glial cells. Repeated, but not single, METH treatment also induced TIMP-2 mRNA and protein expression, and the TIMP-2 was expressed in neurons (19). Some previous

Table 1. Summary for changes in MMP/TIMP levels in the brain induced by METH

	METH treatment	
	Single	Repeated
MMP-2 protein	±	↑
MMP-9 protein	±	↑
TIMP-2 protein	±	↑

±, No change; ↑, Significant increase.

studies suggested that the MMP/TIMP system is expressed in neuronal and glial cells and that the expression level and cellular localization may be regulated according to the developmental and/or functional status of the brain (27, 28). For instance, during the process of axonal extension, MMP is located at the growth cone tips, permitting attachment/detachment between the neurons and matrix substratum (32), and oligodendrocytes utilize MMPs to extend their processes (33), suggesting that the regulation of MMPs is likely to provide guidance during the proliferation of new synapses. Accordingly, it is plausible that MMP-2 and MMP-9 take part in the structural and functional alterations in the brain following repeated exposure to METH.

Role of the MMP/TIMP system in METH-induced behavioral sensitization and reward

We demonstrated that METH-induced behavioral sensitization and conditioned place preference (CPP), a measure of the rewarding effect of a drug, were markedly attenuated in MMP-2 homozygous knock-out [MMP-2-(–/–)] and MMP-9-(–/–) mice compared with wild-type mice (18). We found that inhibitors of MMP-2/-9 blocked the METH-induced behavioral sensitization and CPP (19). Antisense TIMP-2 oligonucleotide (TIMP-AS) treatment, which inhibited the METH-induced increase in TIMP-2 protein expression, enhanced the sensitization, an effect that was associated with a potentiation of the METH-induced release of dopamine in the NAc (19). Accordingly, it is suggested that the net increase in MMP activity is responsible at least in part for the development of METH-induced behavioral sensitization, and that the MMP/TIMP imbalance may influence the structural and functional changes in the brain, related to METH dependence. Indeed, the inhibition of MMPs alters functional and structural correlations of deafferentation-induced sprouting such as remodeling in the dentate gyrus of the hippocampus (34). In a behavioral study, MMP-9 knock-out mice displayed impairments in LTP and hippocampal-dependent memory in a fear-conditioning memory task (30). Since learning/memory mechanisms are considered to overlap with and are involved in the development of drug dependence that occurs with the chronic administration of drugs of abuse (2, 8), MMP-2 and MMP-9 expression may play a crucial role in the acquisition of METH-induced CPP. Interestingly, Brown et al. (35) have demonstrated that MMPs were involved in the learning of a cocaine-associated contextural memory and that reconsolidation of this memory was disrupted by an MMP inhibitor. Furthermore, they showed the ability of an MMP inhibitor to impair the expression of memory for a cocaine-associated cue after extinction. Although they did not examine whether MMP activity and expression were increased by cocaine treatment or a cocaine-associated stimulus, MMPs may also have a crucial role in drug-associated memory.

Role of the MMP/TIMP system in dopamine neurotransmission

Behavioral changes induced by METH are linked to its capacity to elevate extracellular dopamine levels through the redistribution of dopamine from synaptic vesicles to the cytosol and promotion of reverse transport (7, 36). METH-induced behavioral sensitization is associated with an enhancement of the METH-induced increase in extracellular dopamine levels in the NAc (7, 15). In the MMP-2-(–/–) and MMP-9-(–/–) mice compared with the wild-type mice, METH-increased dopamine release in the NAc as well as METH-induced behavioral sensitization and CPP were attenuated. TIMP-AS treatment enhanced the sensitization of METH-induced dopamine release in the NAc, while MMP-2/-9 inhibitors reduced it. In contrast, infusion of purified human MMP-2 into the NAc significantly potentiated the METH-increased dopamine release. The uptake of [^{3}H]dopamine into striatal synaptosomes was reduced in wild-type mice after repeated METH treatment, and the changes in [^{3}H]dopamine uptake were significantly attenuated in MMP-2-(–/–) and MMP-9-(–/–) mice (18). It has been demonstrated that the reverse activation and internalization of plasmalemmal dopamine transporter (DAT) are involved in the METH-induced increase in extracellular dopamine levels (36, 37). These results suggest that both MMP-2 and MMP-9 play a crucial role in METH-induced behavioral sensitization and reward by regulating METH-induced dopamine release and uptake via DAT in the NAc.

The sensitivity of dopamine receptors to endogenous and exogenous ligands is important for dopamine neurotransmission in physiology and pathology. Reduced signaling via Gi-coupled receptors may be an important neuroadaptation in cocaine addiction (38). G protein signaling in the Fc plays a crucial role as a potential pathological change contributing to cocaine sensitization and drug seeking (39). In fact, we also have shown that dopamine receptor agonist–stimulated [^{35}S]GTPγS binding was reduced in the Fc of rats sensitized to METH. TIMP-AS potentiated, while a MMP-2/-9 inhibitor attenuated, the reduction in dopamine D_2 receptor agonist–stimulated [^{35}S]GTPγS binding. Repeated METH treatment also reduced dopamine D_2 receptor agonist–stimulated [^{35}S]GTPγS